CONF-761012--39

TRANSFER AND FOCUSING OF HIGH CURRENT RELATIVISTIC ELECTRON BEAMS ON A TARGET

E. I. Baranchikov, A. V. Gordeyev, Yu. V. Koba, V. D. Korolev, V. S. Penkina, L. I. Rudakov, V. P. Smirnov, A. D. Sukhov, E. Z. Tarumov and Yu. L. Bakshayev

Paper at the Sixth IAEA Conference On Plasma Physics and Controlled Thermonuclear Reactions

(FRG, Berchtesgarten, October 6-13, 1976)

Translator: Joseph Crabbs

TECHTRAN CORPORATION
Post Office Box 729
Glen Burnie Maryland

Studies conducted in the Soviet Union on initiating pulsed thermonuclear reactions in envelope-targets using relativistic electron beams (REB) [1] have a two-fold purpose: a study of the physics of the processes occurring in targets and possibilities of transferring the energy of high current REBs to its surface. Work on the first problem involved following successes in focusing high current beams in the diodes of existing accelerators [2, 3, 4]. Their further development is closely tied to the search for effective methods of focusing more powerful beams to obtain energy currents $\gtrsim 10^{13}$ W/cm^2. Research in recent years on focusing high current beams in diodes shows that beams with energies up to 10 kJ are effectively focused in the anode on a spot of several millimeters, with current densities up to 10-30 MA/cm^2 [2]. Although at the present time there exists no well-defined interpretation of phenomena in high current diodes, the presence of well-focused beams has made it possible, due to the high current density and power, to conduct experiments on accelerating thin foils to velocities of $\lesssim 10^7$ cm/sec, compressing and heating deuterium plasma in a multienvelope target to thermonuclear temperatures [5, 6]. The search for means of increasing power and energy in focused REBs must be continued.

Recently the transfer problem has acquired great significance; this problem can be solved by exploding targets with an energy release of more than 10^7-10^8 J [7]. This level of energy release is of interest for pulsed thermonuclear reactors.

Research is being conducted at the present time in the I. V. Kurchatov Atomic Energy Institute to investigate possibilities of creating a pulsed thermonuclear reactor based on REBs; this work involves the creation of a multimodel system using vacuum lines for transferring energy and an acute angled external magnetic field for transferring electron beams to the target [7]. A field of this configuration can be used at the same time for accumulating a "cloud" of relativistic protons around the target for purposes of irradiating them. This alternative solution of the problem of target irradiation, instead of focusing beams directly on it, may prove to be highly promising. Experiments are described below which were conducted recently on high current electron accelerators "URAL", "MS" and others and which were directed at investigating possibilities of transferring and focusing high current REBs, as well as effective transmission of electromagnetic energy using vacuum lines at considerable distances.

§1. Injection In Transfer of a Disk Relativistic Electron Beam Into an Acute-Angle Magnetic Trap

Experiments in simulating radial transfer and accumulation of an electron cloud are being conducted on the high current accelerator "URAL" adapted for generating and injecting a disk beam with an energy of approximately 500 J (electron energy 200-300 kev, beam current approximately 50 kA, pulse duration 60-70 nsec) into a magnetic trap with acute field geometry through its equatorial slit [7, 8].

A diagram of the experiments is shown in Figure 1. A plexiglas cup 80 mm in diameter (1) is inserted into the high voltage diode cathode holder of the accelerator; this cup has a circular slit in the equatorial plane of the magnetic trap (3) 10 mm in diameter which is sealed with aluminum foil 12-15 microns thick connected to the housing of the unit with a copper foil strip which served as the anode of the accelerator gap.

Cathode 2 was a stainless steel ring with an opening of 86 to 92 mm in diameter and a thickness of from 0.5 to several millimeters. A cathode with a tapered edge was used in a number of the experiments. The disk beam was injected through the anode foil in which a hole was burned 1.5 to 4 mm wide, depending on the experimental conditions, in particular, on the strength of the trap magnetic field in the region of the beam injection. A photograph of a cup after the experiment is shown in Figure 2. A pulsed magnetic field (current period 10 μsec) of acute geometry (3) was created using two copper screws (4) with countercurrents in them. The distance between the screws was 20 or 40 mm. Maximum field strength in the trap slit and plugs at the instant of beam injection, with L = 40 mm, was 13 koe and 6 koe respectively. The sizes and configuration of the screws in the magnetic field are shown in Figure 3.

We conducted experiments on transferring energy with an electron beam to a target located at the center of the magnetic trap with residual air pressure in cup (1) from $4 \cdot 10^{-4}$ torr to several torr.

The energy of the beam of the diode was determined from the voltage and current oscillograms with correction for the inductive component of the voltage. Typical voltage and current oscillograms in the diode and the x-ray radiation detector signal are shown in Figure 4. For ordinary conditions the energy of the beam determined by this method was 470-480 J.

Along with this, the energy of the electron beam behind the anode foil was determined with various forms of thin-walled graphite calorimeters. A photograph of the calorimeter which consists of two graphite disks 50 mm in diameter located in a plane with the two trap plugs is shown in Figure 5. The calorimeters were protected by radiators of thin aluminum foil (10 μm) to preclude heat radiation in case of local overheating of them. Calorimetric measurements showed that the beam is injected in a symmetrical manner with less than 10% scattering. The total energy evolved at the calorimeters with the target absent in the center of the trap for the magnetic field in the slit H_{trap} = 13 koe (L = 40 mm) and pressure $4 \cdot 10^{-4}$ torr, was 415-420 J under ordinary conditions. Calculation shows that the energy loss by an electron beam in one pass to the anode foil is on the average almost 5%, allowing for energy spectra. Comparison of calorimeter readings with the total energy of the electron beam in the diode indicates the absence of multiple (> 5-10) passes of most of the electrons through the anode foil. When the pressure in the cup is reduced to 1 torr, the total energy determined from the calorimeter reading drops no more than 10-15%.

Distribution of the heat evolved at these calorimeters was also studied in this work in the absence of a target in the center of the trap, depending on the position of the beam injection plane. In these experiments to more specifically fix the injection plane, the electron beam was collimated by a circular slit 1 mm wide which was formed between two stainless steel cylinders 100 microns thick which were slipped on the top (1), and a circular cathode 5 mm thick was used. Results of experiments show that when the injection plane (plane of the collimator) is shifted out of the equatorial plane of the trap, the readings of the "far" calorimeter (calorimeter from which the collimator was moved) dropped, and when shifted 2 mm showed 40-50% of the readings of the other calorimeter, and when shifted 3 mm 30-35%. These results, in actuality, did not depend on the pressure in the cup when it was changed from $5 \cdot 10^{-4}$ to 1 torr. The total energy recorded by the calorimeters or a collimated electron beam was nearly 50% of the total beam energy determined from the

voltage and current oscillograms; this recorded energy depended little on the position of the injection plane within the limits of the collimator shift (up to 3 mm). Let us note that the medium Larmor radius for electrons passing through anode foil in the region of the trap slit magnetic field ($H_{slit} \approx 13$ koe) was ≈ 0.8 mm; this precluded direct incidence of electrons on the far calorimeter when the collimator was shifted more than 1.3 mm. Consequently, it can be assumed that when the collimator is shifted 2 mm or more, the readings of the far calorimeter are due to the incidence of electrons on it which have been "captured", i.e., which have passed through the central region of the trap. If it is assumed that the captured electrons completely forget the prehistory of their movement during nonsymmetrical injection, it can be assumed that the quantative captured electrons incident on both collimators should be the same. By using experimental data on the distribution of heat evolved on the calorimeters, it can be found that, when the injection plane is shifted 2 mm, a part of the energy carried by the captured electrons is approximately 60% of the total energy evolved at the calorimeters, and in the case of a 3 mm shift, this fraction drops to 50%. Estimations show that the fraction of captured electrons during injection of an uncollimated beam in the equatorial plane using a cathode 1 mm thick will be at least 60-70%.

The energy transmitted to the target located in the center of the magnetic trap was determined from measurements of matter sublimation and heating of the various test pieces irradiated by a flow of relativistic electrons. Heating of the pieces was measured using a thermocouple (5), and sublimation by the decrease in mass following the experiment. It should, however, be kept in mind that the energy determined from thermodynamic sublimation is low without considering ionization of vaporized matter. There is also another source of errors associated with splitting off of microparticles carrying electron irradiation of the targets; this source of error plays a significant role at energy current densities greater than 10^{10} W/cm^2 and results in overestimation of the energy determined from mass loss [9]. Too more reliably establish the energy evolved on the targets, the measurements were taken using various test bodies made of graphite, aluminum, copper and lead (globules 4, 6, 8 mm in diameter and cylinders 8 mm in diameter and 6 mm long) considering available data on kinetic sublimation and data on the splitting off of microparticles. The medium energy current density on the surface of the test pieces in the center of the trap in our experiments did not exceed $(2\text{-}3)\cdot 10^9$ W/cm^2 and therefore corrections associated with the splitting off effect of microparticles did not exceed 20-30%. The results of measurements show that, in the case of low residual air pressure ($\leqslant 10^{-3}$ torr), for a magnetic trap with L = 40 mm and H_{trap} = 13 koe not less than 30% of the initial energy confined in the beam released at the targets with a surface area of 2 cm^2 (globule diameter 8 mm). When the pressure is increased to several torrs, the fraction of energy released at the targets of these dimensions increases to 35%. When the magnetic field is halved (H_{trap} = 6.5 koe) a small increase in energy released at the trap is observed (10-15%).

The nature of beam propagation in the trap and the degree of homogeneity of target irradiation were determined in these experiments. The beam trail in x-ray beams was photographed with a camera obscura to establish the propagation nature of the disk electron beam in the trap (6). Photographs from various regions of the trap made with a tantalum converter (cylindrical

or conical) with approximately 1 torr pressure in the cup are shown in Figure 6. It can be seen from the photographs that the beam preserves its disk shape in passing 20 mm radially into the trap. Finally, nonuniform luminescence of the lead globule 8 mm in diameter suspended on a fine wire in the center of the trap is clearly visible in the last frame of Figure 6 (pressure P = 4 torr). With low pressure ($P < 10^{-3}$ torr) the nature of beam propagation is different. X-ray luminescence of the surfaces of test pieces inside the trap is essentially more uniform than at high pressures; this indicates "scattering" of the beam. The radiation symmetry and high level of energy transfer effectiveness to the target in a case of scattering of the beam which has entered the trap can be explained by the fact that the magnetic field used is a good trap for relativistic electrons; the equatorial slit of this trap is blocked by electrical and magnetic fields in the diode, and the loss area through the plugs is small. In this trap the relativistic electrons entering it should accumulate in the form of a "cloud" in the region of the neutral pole. If the target falls into this cloud, its surface will be uniformly heated by the relativistic electrons being injected into it.

§2. Vacuum Line Wave Mode With Magnetic Insulation

Earlier work on magnetic self-insulation of vacuum lines l = (0.4-0.7) m long were performed under conditions cT_f/l 10-15 (where T_f - duration of the pulse front at the line input, in seconds) [10]. Meanwhile, the length of the lines should be approximately (3-5) m, $T_{f/l} \lesssim 3$ for the accelerator with beam energy 10^7 J. Therefore the shaping of the wave front with magnetic insulation and the effect of possible leakage currents on the effectiveness of energy transfer from the accelerator to the diode must be investigated.

The results of studies conducted on accelerator "MS" with a coaxial line with external and internal stainless steel electrodes 5.2 cm and 2.0 cm in diameter and 3.5 m long are given below. In the experiment whose diagram is shown in Figure 7, the voltage and current at the input and current to the Faraday cylinder, and end anode, and the x-ray radiation from the anode and side line walls were measured. The pressure of the neutral gas at the input into the line was $5 \cdot 10^{-6}$ torr and 10^{-4} torr at the anode. The accelerator gap varied from 0 to 1 cm.

When E ~ 200-250 kV/cm an explosive emission from the negative electrode occurred at the voltage pulse front; this was noted from discontinuities on the voltage and current oscillograms. Up until this time an ordinary electromagnetic wave was propagated along the line. In order to reduce its intensity, a dielectric insert 4 cm long was placed at the input into the line in a number of experiments, or part of the internal electrode 20 cm long was covered with a film of Aquadag [Translator's Note: a graphite lubricant] to reduce the delay time of the explosive emission occurrence. It is apparent from typical current and bremstrahlung oscillograms (Figure 8) that there is a forerunner with low amplitude behind which the main front begins. The propagation speed of the forerunner is equal to the speed of light. The use of dielectric inserts and Aquadag covering of the electrodes at the input of the line resulted in a sharp decrease in the amplitude of the forerunner (Figure 9); this indicates a relationship between its appearance and the absence of intense emission from the negative electrode at the beginning of the pulse. The wave propagation along the line resulted in

distortion of the main front. As follows from Figure 9, the current buildup velocity in the Faraday cylinder tripled in comparison to the shunts; it was $2.4 \cdot 10^{12}$ A/sec. The propagation speed of the main pulse front was low (0.45 $\pm$ 0.05) sec for the voltage pulse amplitude at the 460 kV input. Analyses of the oscillograms indicate the strong dependency of front velocity on voltage. In the simplest case wave propagation with magnetic insulation can be described by equations of telegraphy:

$$\frac{\partial U}{\partial z} = -\frac{1}{c}\frac{\partial A}{\partial t} \qquad (1)$$
$$\frac{\partial J}{\partial z} = -\frac{\partial Q}{\partial t} - GU$$

If we consider that the width of the wave front $\Delta \ll l$ and assume buildup behind the magnetic self-insulation front [10, 11], wave velocity can be obtained in the form

$$v = c\sqrt{\frac{\gamma - 1}{\gamma + 1}} \qquad (2)$$

where $\gamma = 1 + \frac{eU}{mc^2}$

The values of v found from (2) are near experimental values.

The characteristic feature of the wave solution with magnetic insulation lies in the great losses compared to the quasistationary state. The overall leakage charge depended on the current and voltage, and as follows from Figure 10, was minimum for d = 2 mm. Leakages to the side wall of the line generated x-ray bremstrahlung with an energy corresponding to the voltage in a line. Rough estimations of the leakage charge from x-ray measurements are at least 30% of the charge flowing onto the anode.

Among the probable causes of leakage, let us note losses on the wave front which follow from the ideas developed above, geometrical heterogeneity and possible instability of the electron layer in the gap. The effect of these factors can be reduced by choosing a mode with a greater current than that which follows from the theory of magnetic insulation.

§3. Focusing an Electron Beam in Lines With Magnetic Insulation

When the strength of the electric field in the gap is increased to 2-3 MV/cm, the formation of a focused beam which propagates in the end gap of the coaxial cable at a distance of from 0.3 cm to 2.0 cm was observed.

These measurements were conducted on the "MS" unit in a line 10 cm long which operated in the quasistationary mode. Coaxial cables with an external radius of from 0.2 to 2.5 cm and internal radius of from 0.035 to 0.2 cm were mounted at the output of the accelerator tube. The length of the coaxial cable varied from 1 cm to 10 cm, while measurements have shown that the impedance of the coaxial cable did not in actuality depend on its length.

It follows from analyzing the oscillograms that for b/a = 0.4/0.2 the current to the Faraday cylinder is delayed relative to the beginning of the current at the shunt by ~ 34 nsec when the gap is increased from 0.3 to 2.0 cm. It can be confirmed with up to 10% accuracy that the time delay ΔT increases linearly as gap d increases.

The effectiveness of beam transmission, which is determined by the ratio of charges incident on the Faraday cylinder and passing through the shunt, is shown in Figure 10 for a change in the gap. In doing this the current on the lateral surface of a coaxial cable in its end section increases; this is also confirmed by measurements of x-ray radiation from the lateral surface. The beam transfer condition to the coaxial cable is determined by its impedance. For a highly cylindrical form $b/a \gg 1$ an approximated calculation gives an impedance value $Z \sim T/s = 30\ \Omega$.

The drop in impedance of a coaxial cable and its time displacement can be explained by the formation of plasma in the diode gap. In fact, a high plasma concentration is formed on the internal electrode of the coaxial cable as a result of stripping of micropoints. In large diode gaps the current is initially incident on the lateral surface of the higher coaxial cable, as a result of which the plasma is accelerated in a longitudinal direction and injected into the diode gap [12]. In doing this the main part of the beam is incident on the Faraday cylinder. The time delay of the current on the Faraday cylinder gives a plasma velocity value of approximately $5 \cdot 10^7$ cm/sec (Figure 12). To estimate the density of the plasma injected into the gap a hydrodynamic equation can be used:

$$M \frac{\partial V_z}{\partial t} = - \frac{\partial}{\partial z} \frac{H_\varphi^2}{8\pi}$$

The expression

$$n \simeq \frac{H^2}{8\pi M V_z^2} \sim \frac{M_H}{M} \cdot 3 \cdot 10^{13}\ \text{см}^{-3}$$

is obtained for the plasma density from this formula. It is essential that this density be of the same order as the beam density, on the condition that the beam size is determined by the size of the focused spot on the anode. The presence of this plasma is confirmed also by the short-circuiting of the diode gap with gaps $d < 2$ cm for a time less than pulse duration, recorded from the characteristic "pulling" of the current to the Faraday cylinder. The distribution of beam current density on the anode obtained by a camera obscura is given in Figure 13. The focusing region is 1 mm for half the height. The measurements of bremstrahlung intensity with a scintillation meter using a collimator system with 8, 4 and 2 mm apertures established that 90% of the overall x-ray radiation from the end passes from the 8 mm diameter opening, 35% of the radiation from the 4 mm diameter opening, and 20% of the x-ray radiation from the 2 mm diameter opening. In doing this the average current density in the focusing region is 0.5 MA/cm^2. The electron energy determined from the hardness of the x-ray radiation corresponds to the voltage in the anode. Let us note that focusing in coaxial geometry produces a softer generator-load connection.

§4. Focusing a High Current Electron Beam in a Diode Using a Pin

We have previously recorded the results of acute and effective focusing of a beam in the high current accelerator "Ural", with wave resistance of the shaping line ρ = 2.5 Ω using a pin attached to the cathode [2]. As has been noted in [2], the attempt to describe the focusing phenomena using a pin on the basis of parapotential theory has not been well grounded. The results have depended little on the length of the pin, or in other words, on the ratio of the diode radius to the distance of the cathode-anodes. On the other hand, focusing depended a great deal on the gap between the pin and anode.

Additional experiments were conducted on the accelerator "Ural" to investigate the pin focusing mechanism; studies were also conducted on another high current accelerator with parameters considerably different from those of the "Ural", primarily a difference in the resistance of the shaping line of approximately 0.3 Ω. A schematic view of this accelerator is given in Figure 14. The electrical length of its water coaxial line was 30 nsec, with a rated power reserve of approximately 100 J. A voltage of 40-60 kV was sent to the accelerator diode through a gas commutator. Typical current, voltage and x-ray radiation oscillograms for two gap values (d) between the pin and anode are shown in Figure 15. Gap d = 1.5 mm is the optimum value, and when d = 0.5 mm a near short-circuit mode was observed in the diode. Photographs of the spherical spotting x-ray light obtained using the camera obscura for an optimum gap d = 1.5 mm are shown in Figure 16. The current density in the 0.5 mm diameter focal spot was 25 MA/cm^2. Focusing with a spot with a complex structure was observed in some of the experiments (Figure 16b).

The hardness of the x-ray radiation emerging from the focal spot was measured on accelerator "Ural" using the method of filters and a lead collimator with a 1 mm diameter aperture attached in the region of beam focusing on the anode. It was established that the hardness of the radiation corresponds to the active voltage at the diode beyond the region of sharp current increase (see Figure 17). It can be concluded from these measurements that focusing in the diode of "Ural" begins due to current breakdown and voltage drop. It can be seen from the curves of Figure 17 that focusing occurred principally when the voltage was near 90-100 kV and the diode current was 100 kA. The focusing time determined from the duration of the active voltage plateau at the diode was somewhat less than the electrical length of the shaping line of accelerator "Ural" (50 nsec) and was 35-40 nsec.

Studies on focusing using a pin which were conducted on both accelerators showed that, in spite of the essential difference in accelerator parameters and their designs, the principal features of the physical processes in them were alike.

From our point of view, the principal characteristics of focusing high current electron beams by pins (spatial and time), the physical processes associated with it in the diodes, and the special features of current, voltage and x-ray radiation oscillograms can be explained on the basis of suppositions concerning the formation of a double layer between the cathode and anode plasma in the pin-anode gap.

Let us turn to a short description of the picture of physical phenomena in a high-current diode during pin focusing of the beam. Diode operation after plasma formation in the pin as a result of explosive emission occurring in the pre-pulsed or principal voltage can be subdivided into test stages: a) vacuum current jump mode (region on the oscillograms up to a sharp current increase, when there exists a vacuum gap between the plasma formed in pin and the anode), and b) "plasma" diode mode, when a double layer is formed between the cathode and anode plasma. It is known [13] that current take-off occurs in the vacuum peak diode mode in accordance with the "3/2" principle, considering the geometry of a single peak:

$I(a) = 30 \cdot 10^{-6} \frac{vt}{d - vt} U_{(6)}^{3/2}$ where v - velocity at the spherically expanding

plasma ($\sim 2 \cdot 10^6$ cm/sec), d - gap, t - time counted off from the instant of plasma formation. As the current increases, the power being liberated at the anode becomes sufficient to form an anode plasma (> 0.5-1 kJ/gr) which begins to expand and moves in the direction of the pin. The "plasma" diode mode is possible only due to the fact that the plasma density and its cross-sectional dimensions in the region where cathode and anode plasma meet (when the initial gap between the pin and the anode is adequately large), the maximum current which can flow in the layer $I_{layer} \simeq enS\sqrt{\frac{T_e}{m}}$

[14] (n - plasma density on the layer boundary, S - effective area of the layer, T_e - temperature of the electrons, m - mass of the electron) is less than the short-circuit current of accelerator $I_{кз} = \frac{U_L}{\rho}$ (U_L - discharge voltage

of the shaping line); this also leads to formation of a double layer and its existence during the applied voltage pulse (u). The thickness of the double layer is determined by the relationship $d_{layer} = 1.3 \cdot 10^{-3} \frac{V^{3/4}(6)}{\sqrt{j_+ (a/см^2)}}$ см

[14], where $j_+ = \sqrt{\frac{m}{M}} \frac{I_{layer}}{S}$ is the ion current density in the layer.

When the plasma density at the layer boundary ceases to change, the thickness of the layer is determined only by the applied voltage. Estimates show that for accelerator "Ural" with the optimum gap between the pin and anode d = 3.5 mm the maximum current in the layer is $\sim$ 100 kA for reasonable assumptions with regard to plasma density based on the data of work [15] n $\sim 10^{16}$ particles/cm^2, electron temperature $T_e \sim$ 4-5 eV [16] and effective emission area S $\approx$ 0.3-0.5 cm^2 determined from the dimensions of the fusion trace which remains on the copper anode. In this case the thickness of the double layer, from an estimate obtained based on the formula given above, is $\sim$ 0.5-1 mm.

One of the principal problems of operating the diode is matching its impedance with the wave resistance of the shaping line. As is apparent from the oscillograms on Figure 13, the optimum gap can be chosen for superior matching. The selection of layer parameters n and S at which

$I_{layer} \approx I/2\ I_{K3}$ apparently corresponds to the optimum gap on the basis of concepts concerning the double layer.

It is known [17] that during spherical plasma expansion the particle density distribution along the radius has the form $n(z) \sim \frac{1}{I^2}$ for $I \leqslant \sqrt{\Delta t}$

where Δt - scattering time. This dependency is confirmed by data on plasma density distribution at the gap axis between the pin and anode obtained in work [15]. According to [15], the plasma density distribution indicates the absence of free scattering of plasma across the axis, beginning with some current in the gap when the pressure of the current magnetic field becomes greater than the plasma pressure and the transverse dimension ceases increasing. By considering the above it can be assumed that, beginning with a certain current, parameter $n \cdot S$ begins to fall as $\sim 1/x^2$, where x - distance along the axis between the pin and plasma boundary. Therefore, I_{layer} can be controlled by selecting the length of gap d. In fact, when the gap is reduced, premature transfer of the diode begins (see the oscillogram of Figure 15, d = 0.5 mm), and when it increases the current in the layer drops and can become considerably less than $1/2\ I_{K3}$, and, in particular, less than the critical current (I_{crit}); this affects beam focusing (see below). When $U_L \approx 500$ kV, I_{K3} is ~ 200 kA. Therefore gap d = 3.5 mm which provides expression $I_{max} \sim 100$ kA is optimum (see curves on Figure 17). It must be noted that the diode impedance with the indicated gap d = 3.5 mm in the region of the voltage plateau is $\approx 1\ \Omega$, which, as has been ascertained, is associated with the response of the single channel water commutator whose resistance was approximately 1.5 Ω with a current of ~ 100 kA.

The electron beam focusing mechanism in this model is determined by the action of the natural magnetic field of the current under vacuum diode conditions as well as during the formation of a double layer, when the current reaches a value exceeding the critical value

$$I_{crit} = 8{,}5\beta\gamma\frac{R}{d_f}(\text{kA}),$$

where R - effective radius of emission surface, in particular, surface of the double layer, and d_f - focusing length. In the vacuum diode mode the focusing length corresponds to a distance between the virtual cathode and anode. When anode plasma is present, focusing can occur not only in the double layer, but in the anode plasma itself, on the condition that the magnetic field with a beam is not balanced in it by the reverse current field. Therefore, in the case of a plasma diode without reverse current in the anode plasma, $d_f \approx d_{layer} + d$ (d_a - dimensions of the anode plasma along the diode axis).

Estimations show that, for accelerator "Ural" with d = 3.5 mm, $I_{crit} \sim 30$-35 kA, on the assumption that $R/d_f \sim 3$-5 and, consequently focusing can begin only from the region of sharp current increase and active voltage drop at the diode; this is confirmed by x-ray radiation hardness measurements. As experience has shown, when gap d is increased to 6 mm, beam focusing completely disappeared, and the current dropped to 10-20 kA. For the other

accelerator (ρ = 0.3 Ω) with d = 1.5 mm focusing should already be beginning in the vacuum current take-off mode ($I_{crit} \sim 4$ kA); this was also confirmed by the absence of noticeable shift of the x-ray radiation pulse which was observed with a collimator attached in the region of the focal spot on the anode.

An important condition for sharp focusing is the timely formation of anode plasma such that the point of encounter of the cathode and anode plasma and layer formation take place at a certain distance from the anode surface; this ensures "crossover" of electron beam on the anode surface in accordance with the picture examined in work [18].

In conclusion let us note that the operation of the high-current diode with pin at the double layer formation stage coincides extensively with the operation of the diode with external plasma injection [19, 20], with the difference that the plasma parameters necessary for normal operation of the diode with the pin are chosen by optimization of the gap. As for focusing a high-current beam, the diode with pin gives better results compared to a low impedance diode with large diameter cathodes, due to the initial localization of the beam current in the region of the gap between the pin and the anode.

REFERENCES

1. Rudakov, L. I., A. A. Samarsky, "6th European Conference on Controlled Fusion and Plasma Physics," Vol. 1, p. 487, 1973.
2. Koba, U. V., V. I. Liksonov, V. S. Pen'kina, L. I. Rudakov, V. P. Smirnov, U. I. Sidorov, A. D. Sukhov and E. Z. Tarumov, "Plasma Physics and Controlled Nuclear Fusion Research," Fifth Conference Proceedings, Tokyo, Vol. 11, p. 337, 1974.
3. Glauser, N. I. et al., "7th European Conference on Controlled Fusion and Plasma Physics," Lausanne, Vol. 1, p. 85.
4. Blaugrund, A. F. and G. Cooperstein, "Phys. Rev. Lett," Vol. 34, p. 461, 1975.
5. Bogolyubskii, S. L., B. B. Gerasimov, V. I. Liksonov, A. P. Mikhailov, Yu. P. Popov, L. I. Rudakov, A. A. Samarskii, V. P. Smirnov, "Discharge of Thermonuclear Neutrons From Plasma Compressed By an Envelope," Reports at the International Conference of IAEA Experts, Dubna, 1976.
6. Rudakov, L. I., M. V. Babykin, "7th European Conference on Controlled Fusion and Plasma Physics," Lausanne, Vol. 2, p. 172, 1975.
7. Baranchikov, E. I., A. V. Gordeyev, U. V. Koba, V. D. Korolev, V. S. Pen'kina, L. I. Rudakov, V. P. Smirnov, A. D. Sukhov, E. Z. Tarumov, "International Topical Conference on Electron Beam Research & Technology," Albuquerque, New Mexico, Vol. 1, p. 284, 1975.
8. Koba, Yu. V., V. S. Penkina, L. I. Rudakov, A. D. Sukhov, E. Z. Tarumov, "Letter in Journal of Theoretical Physics," Vol. 2, p. 312, 1976.
9. Farber, M., J. E. Robin, R. D. Srivastava, "J. of Appl. Phys.," Vol. 43, p. 3313, 1972.
10. Gordeyev, A. V., V. D. Korolev, U. L. Sidorov, V. P. Smirnov, "Annals the New York Academy of Sciences," Vol. 261, p. 668, 1975.
11. Voronin, V. S., A. N. Lebedev, "Journal of Theoretical Physics," Vol. 43, p. 2591, 1973.
12. "Questions of Plasma Theory," Issue 8, edited by M. A. Leontovich, Moscow, 1973.
13. Mesyats, G. A., D. I. Prockurovskii, "Letter in Journal of Experimental and Theoretical Physics," Volume 13, p. 7, 1971.
14. "The Characteristics of Electrical Discharges in Magnetic Fields," Ed. Guthrie, R. Wakerling, New York, 1949.
15. Kelly, J. G. and L. P. Mix, "J. of Appl. Phys.," Vol. 46, p. 1084, 1975.
16. Bakst, R. B., V. I. Manylov, "Bulletin of Institutes of Higher Learning of the USSR, Physics," No. 9, p. 148, 1967.
17. Bugayev, S. P., A. M. Iskoldskii, G. A. Mesyats, D. I, Proskurovskii, "Journal of Theoretical Physics," Vol. 37, p. 2206, 1967.
18. Godstein, S. A., R. C. Davidson, J. G. Siambis, Roswell Lee, "Phys. Rev. Lett.," Vol. 33, p. 1471, 1974.
19. Nedoseyev, S. L., V. P. Smirnov, A. M. Spektor, D. G. Filkin, "Journal of Theoretical Physics," Vol. 42, p. 2520, 1972.
20. Miller, P. A., J. W. Poukey, T. P. Wright, "Phys. Rev. Lett," Vol. 35, p. 940, 1975.

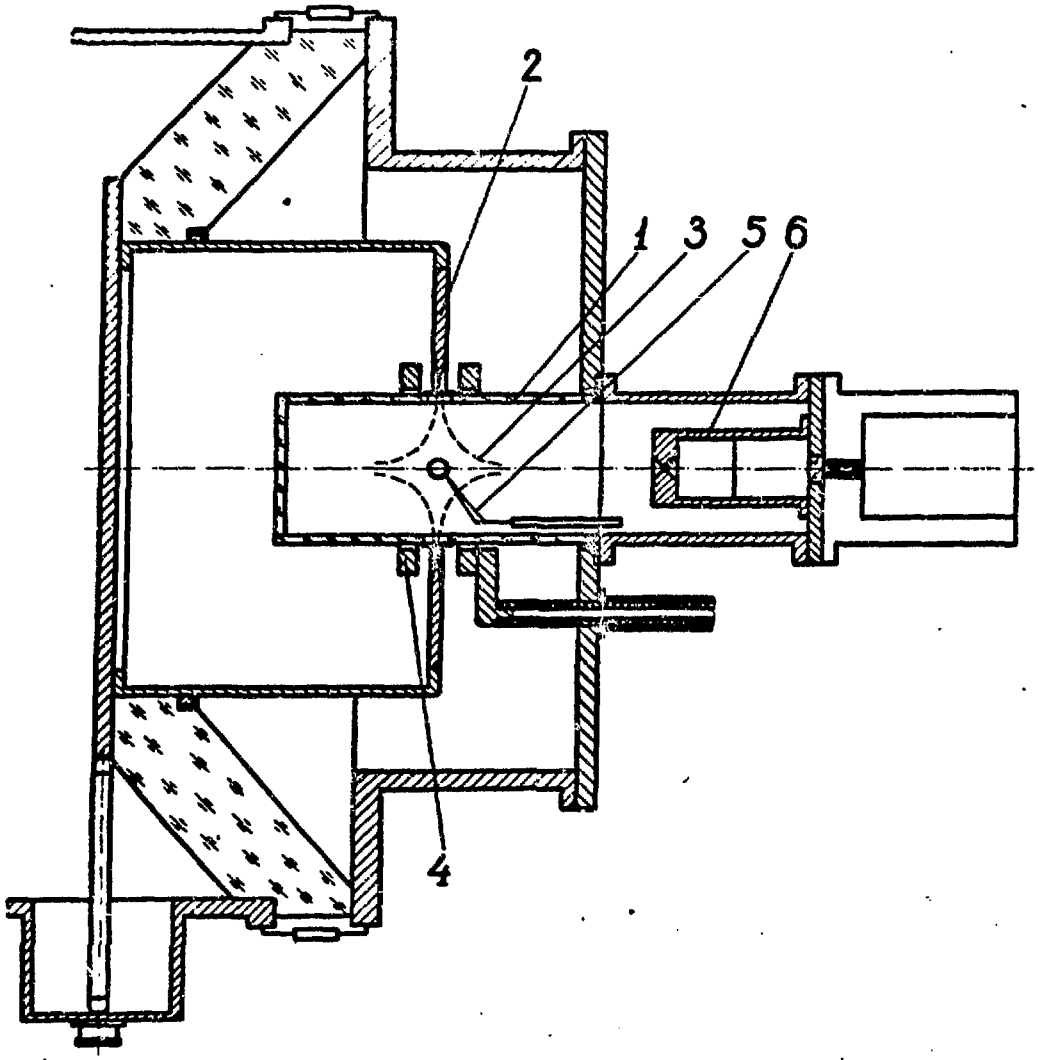

Figure 1. Diagram of the Experiment.

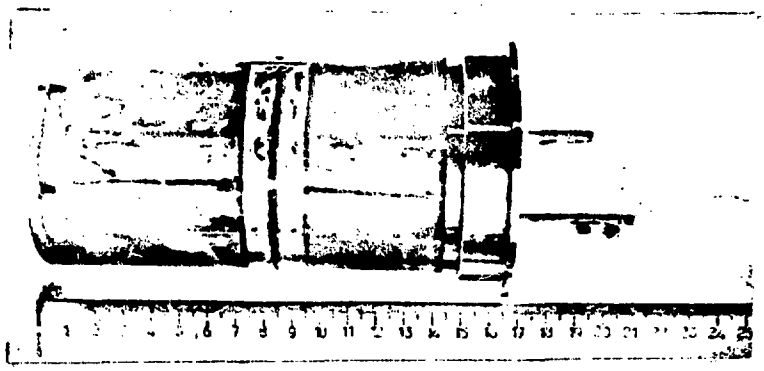

Figure 2. Plexiglas Cup With Circular Slit for Radial Injection of a Disk Electron Beam. The point where the beam has burned through is clearly visible on the anode coil. Width of the burn-through location 1.5-4 mm.

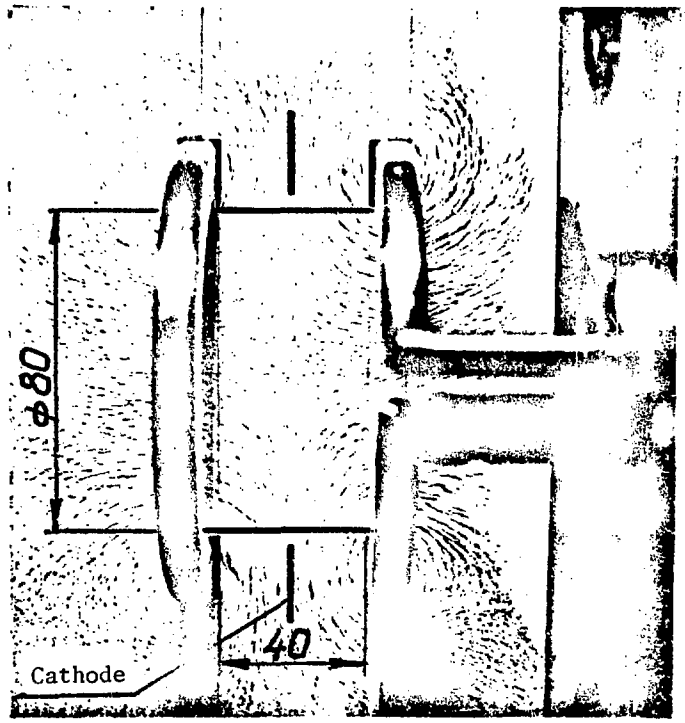

Figure 3. Geometry of the Magnetic Field.

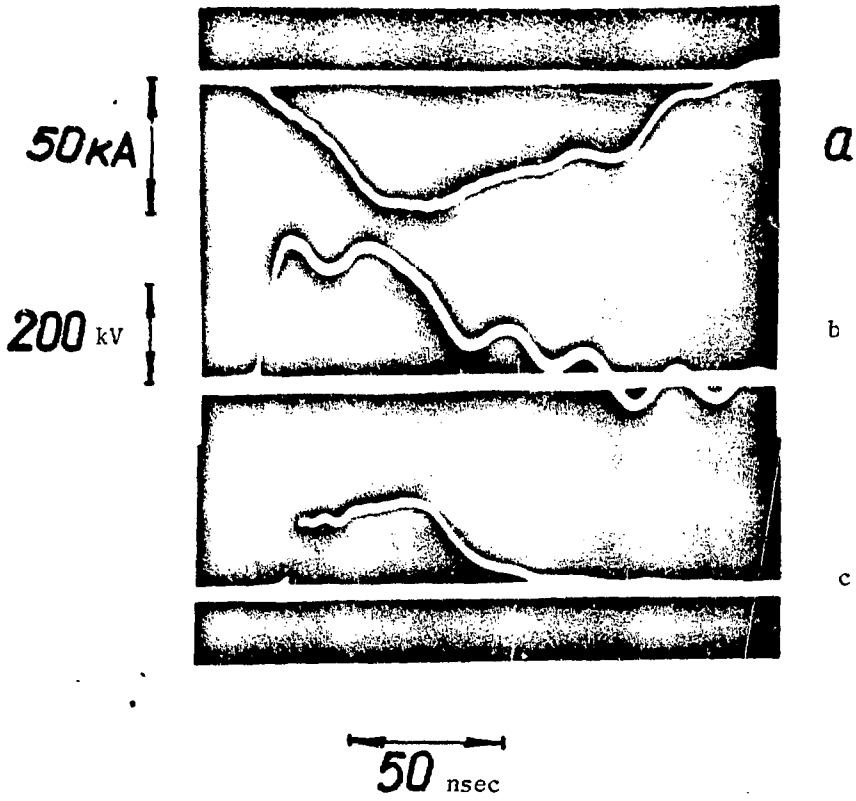

Figure 4. Typical Oscillograms of Current (a), Voltage (b), X-Ray Radiation Sensor Signal (c).

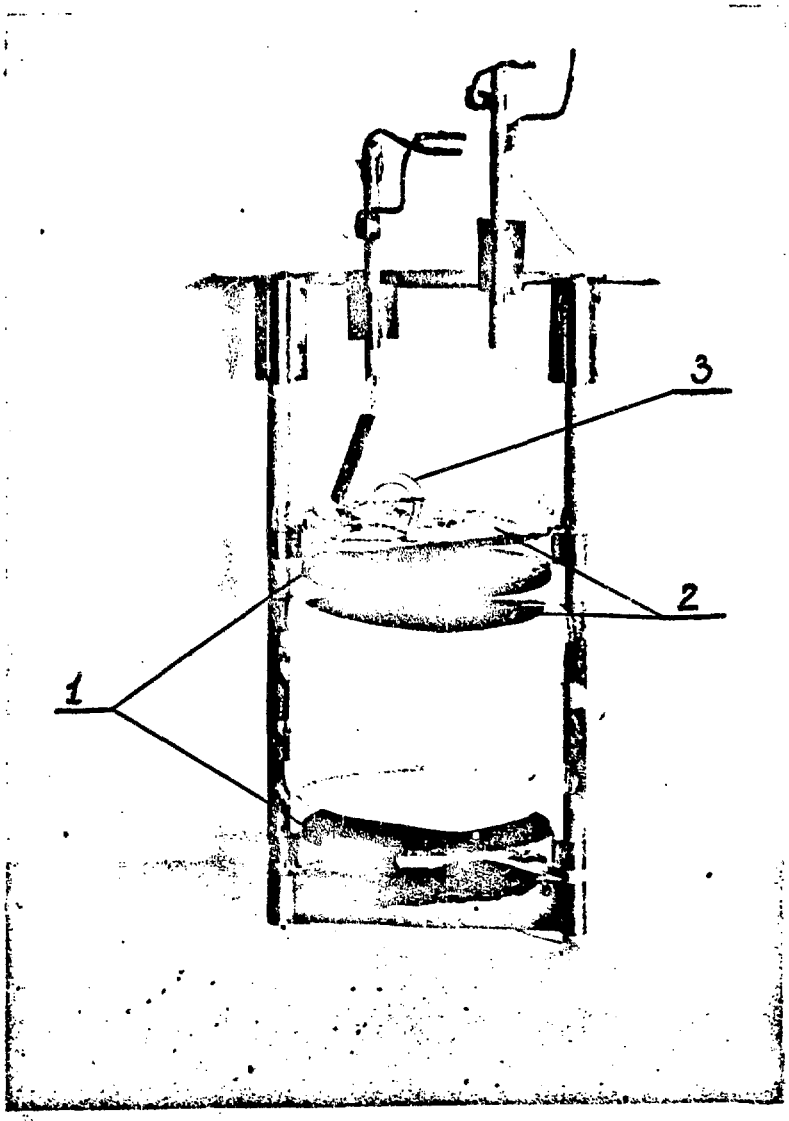

Figure 5. Disk Graphite Calorimeter: 1, Graphite Disks; 2, Radiators (10 μm Aluminum Foil); 3, Thermocouples.

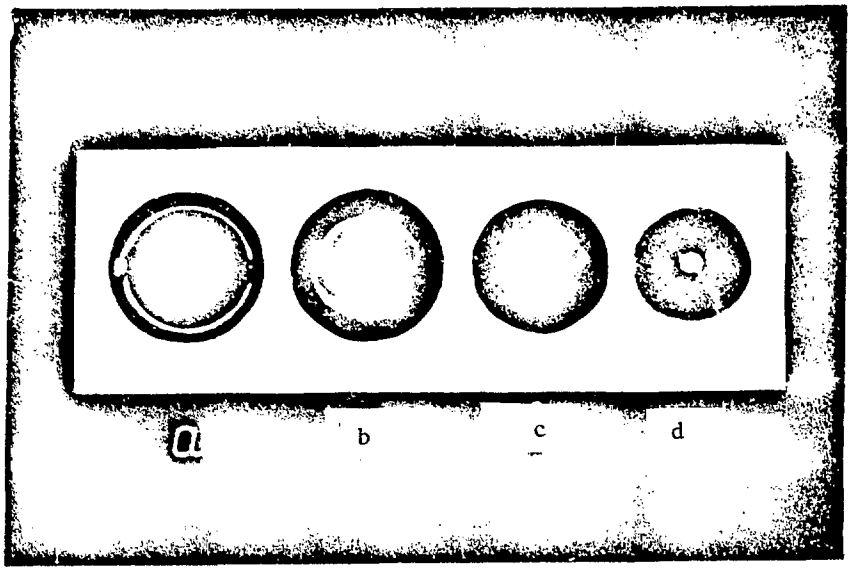

Figure 6. Photograph of Beam Trail In X-Rays.

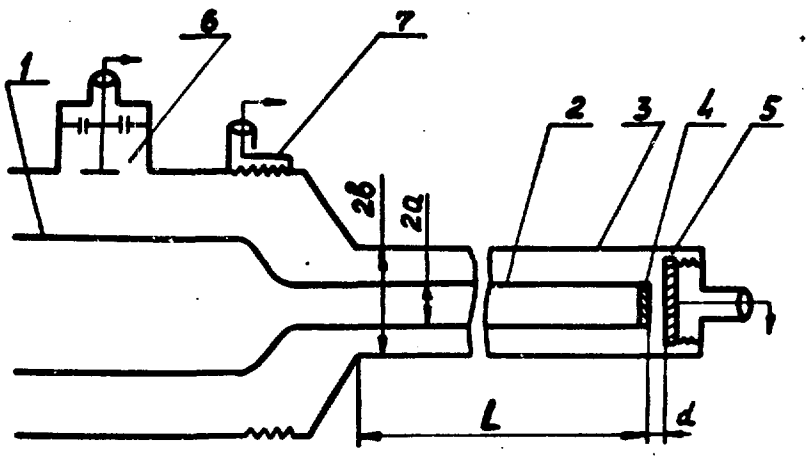

Figure 7. Diagram of the Experiment: 1, Cathode Support; 2, Inner Vacuum Line Tube; 3, Outer Vacuum Line Tube; 4, Cathode; 5, Anode; 6, Capacitive Divider; 7, Shunt.

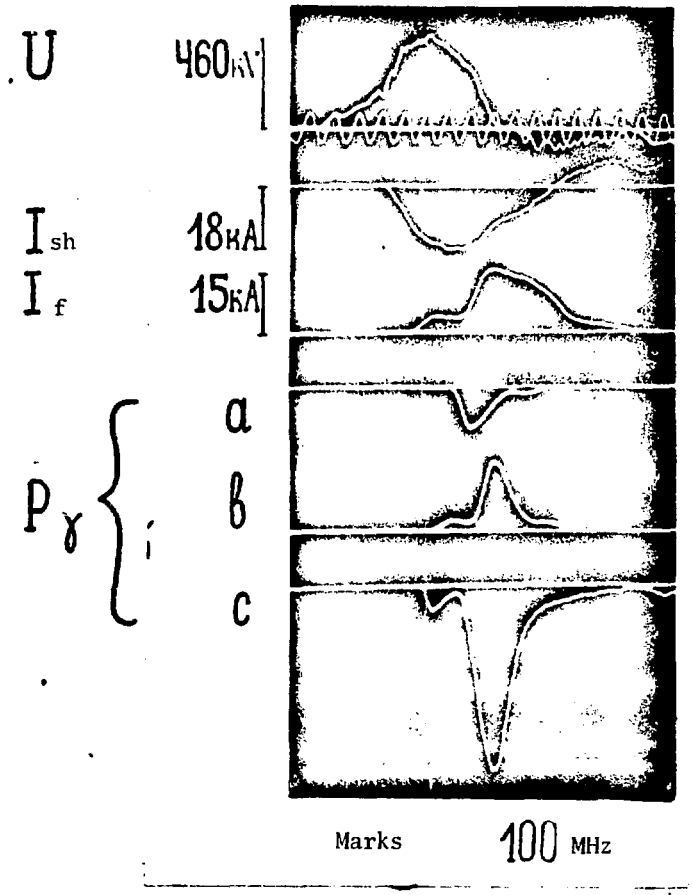

Figure 8. Oscillograms of Voltage (U), Current at the Shunt (I_{sh}), Current in the Faraday Cylinder (I_f), X-Ray Radiation (P_γ) With a Lateral Line Surface: (a) 0.7 m from the Beginning of the Line; (b) From the End of the Line and on the Anode (c).

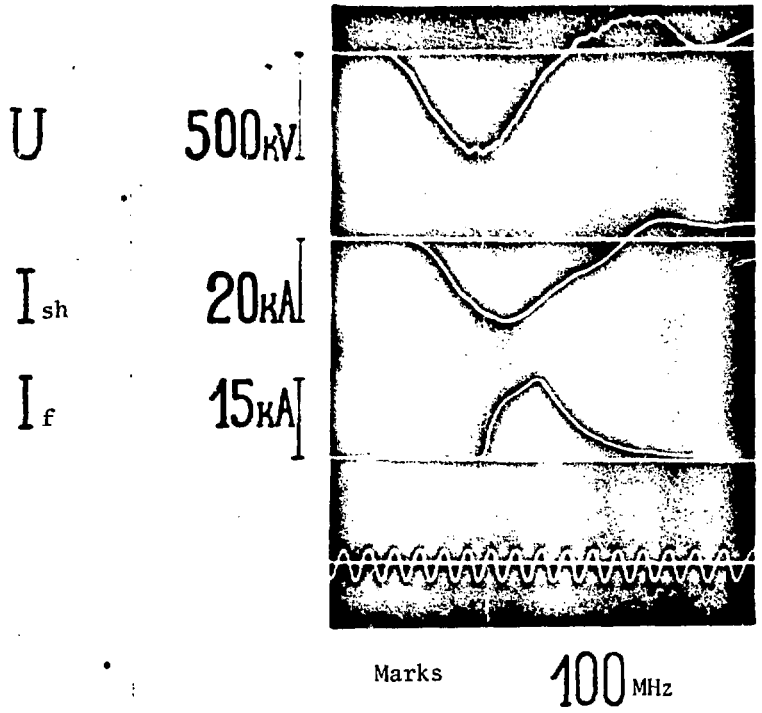

Figure 9. Oscillograms of Voltage (U), Current at the Shunt (I_{sh}) and Current in the Faraday Cylinder (I_f). The initial segment (20 cm) of the Interchannel Electrode Line is Covered with Aquadag.

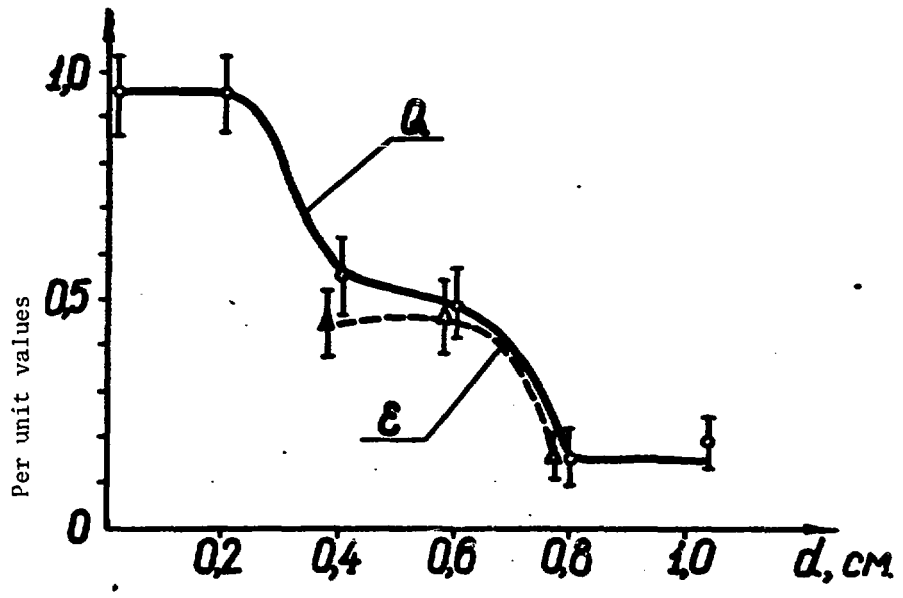

Figure 10. Effectiveness of Charge (Q) and Energy (ε) Transfer from the Acceleration Gap d.

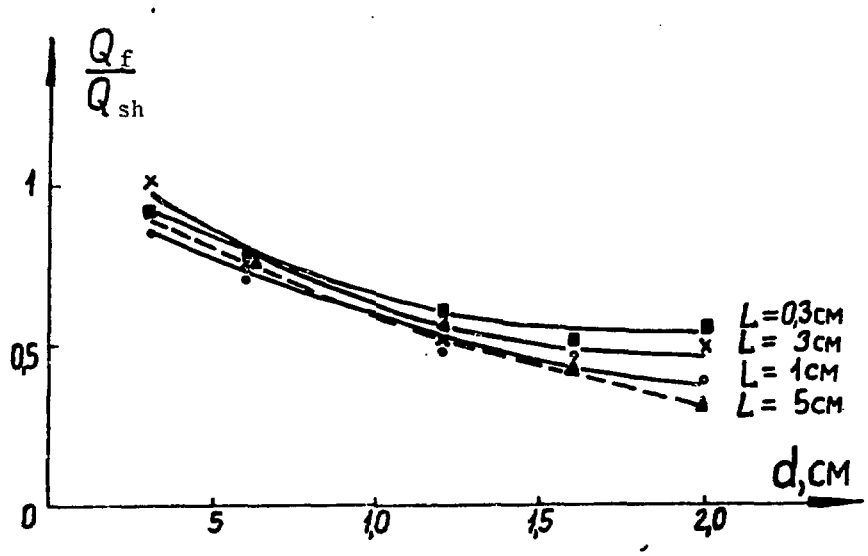

Figure 11. Ratio of Charge Passing Through the Faraday Cylinder to a Full Charge Depending on the Cathode-Anode Gap for Coaxial Cables of Various Lengths (L).

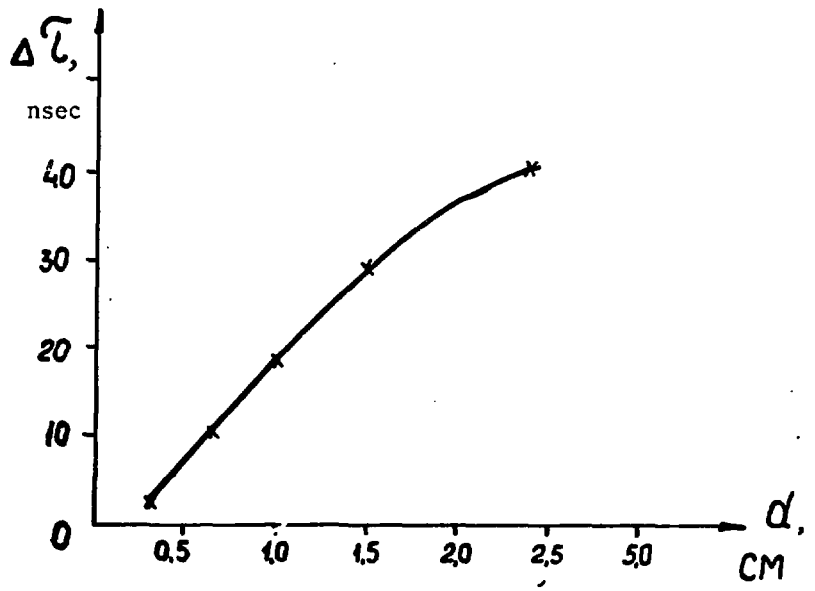

Figure 12. Dependency of Current Delay to the Faraday Cylinder (I_f) on the Accelerator Gap d.

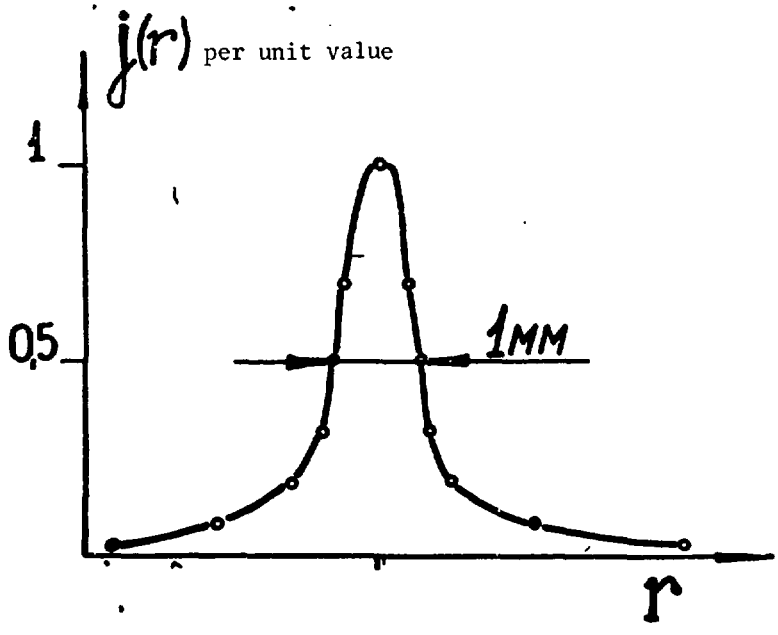

Figure 13. Current Density in the Anode Plane Obtained Using Obscurograms.

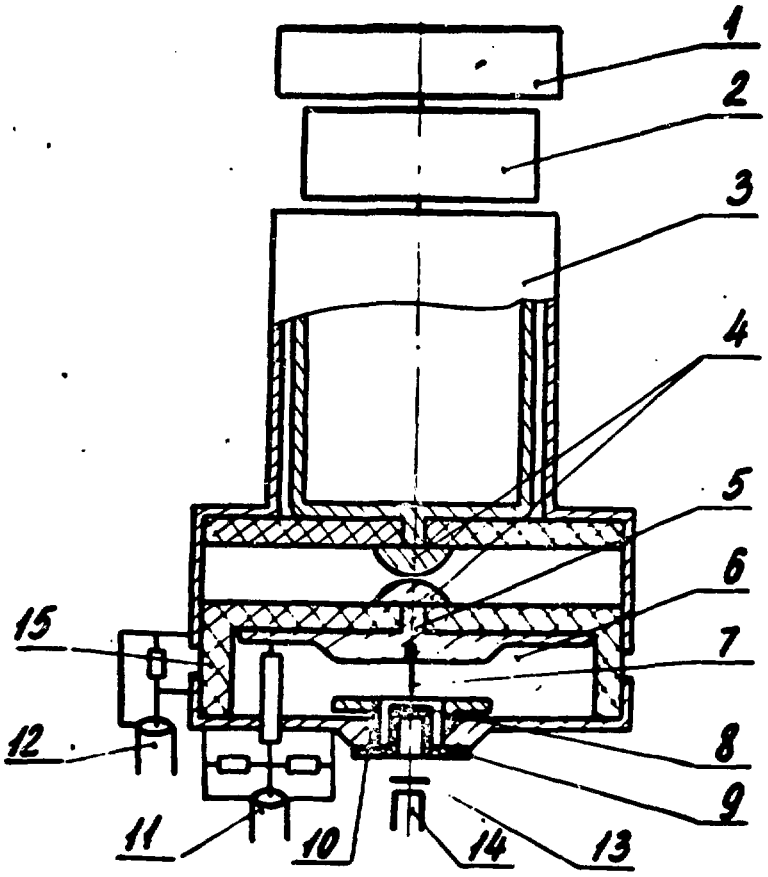

Figure 14. Schematic View of the Accelerator: 1, Energy Storage Capacitor; 2, Controllable Gas Commutator; 3, Shaping Rod; 4, Free Running Gas Commutator; 5, Cathode; 6, High Voltage Diode; 7, Pin; 8, Anode Foil; 9, Anode insert; 10, Anode; 11, Resistive Voltage Divider; 12, Current Shunt; 13, 14, X-Ray Sensors; 15, Polyethylene Diode Insulator.

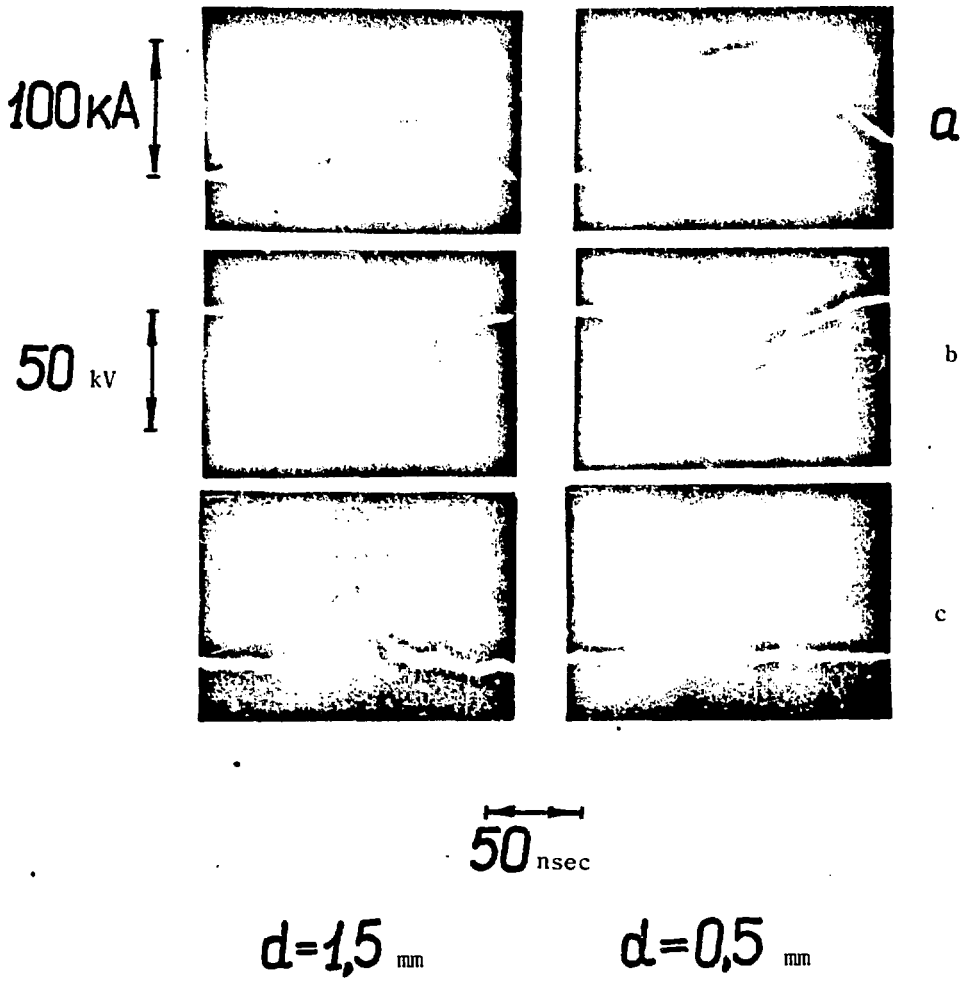

Figure 15. Typical Oscillograms of Current (a), Voltage (b), X-Ray Radiation Sensor Signal (c); I, For Gap d = 1.5 mm (X-Ray Signal 34 Times Weaker); II, For Gap d = 0.5 mm.

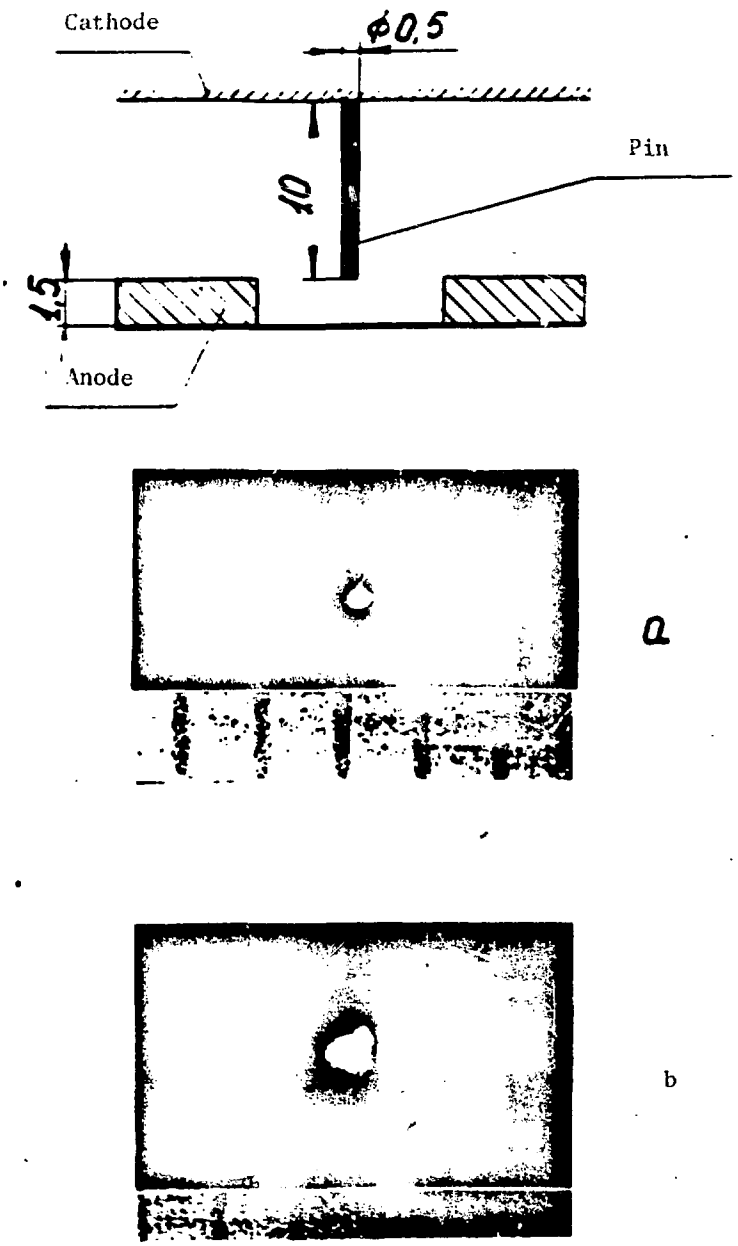

Figure 16. Photograph of the Focal Spot in X-Rays. Photographs obtained using a camera obscura with aperture 0.2 mm. Scale 1:1. a, Normal focusing mode. Tungsten pin, copper anode. b, Structural focusing mode (three focal spots visible). Tungsten pin, aluminum anode 30 μm thick.

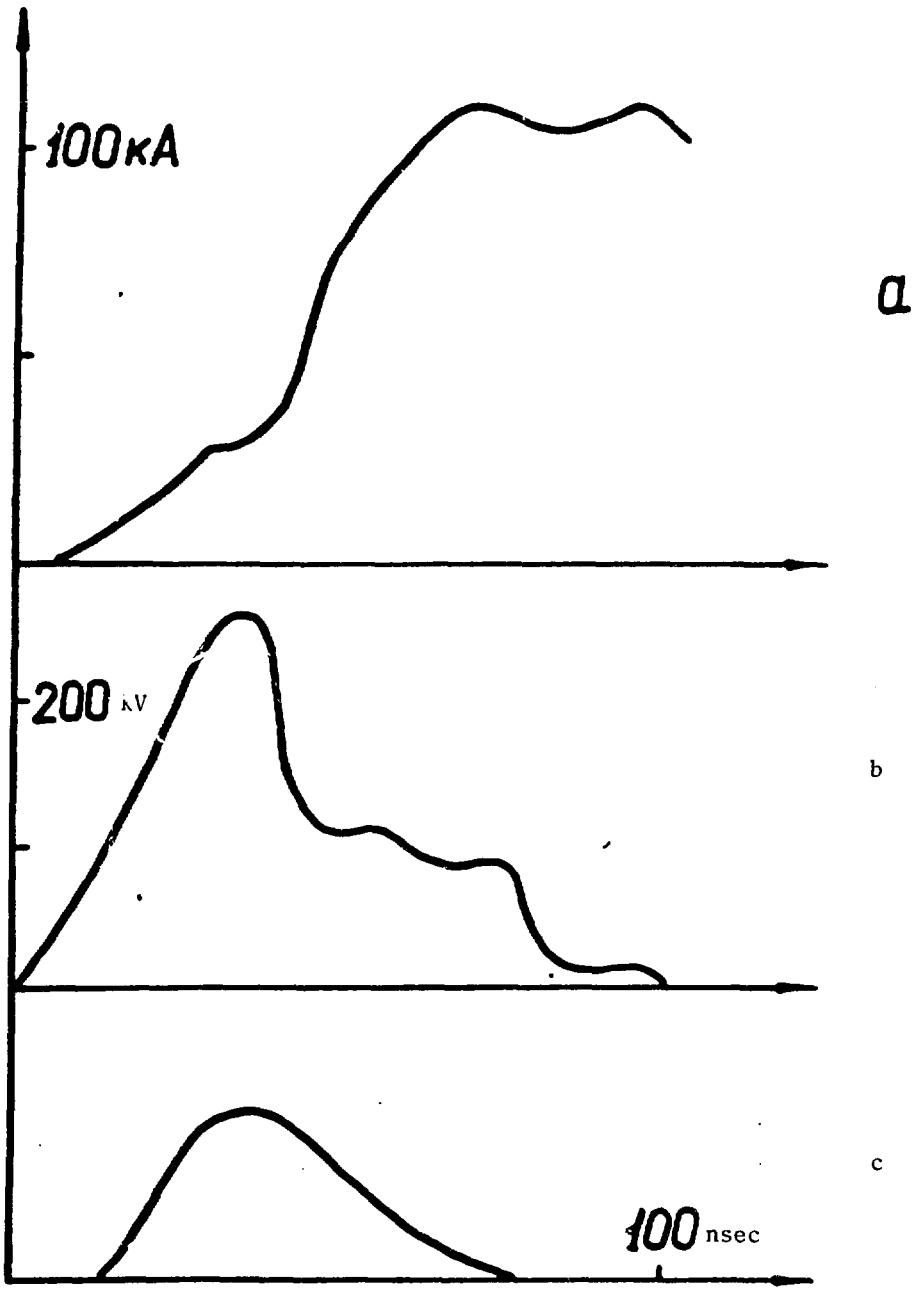

Figure 17. Curves of Current (a), Active Voltage at a Diode (b) and X-Ray Radiation Sensor Signal (c) For Accelerator "Ural" in the Optimum Focusing Mode (d = 3.5 mm).